Mater. Lett.
Jan. 5, 2017

Gas-assisted coating of Bi-based $(CH_3NH_3)_3Bi_2I_9$ active layer in perovskite solar cells

Takayuki Okano[a], Yoshikazu Suzuki[a,b*]

[a] Graduate School of Pure and Applied Sciences, University of Tsukuba, Ibaraki 305-8573, Japan

[b] Faculty of Pure and Applied Sciences, University of Tsukuba, Ibaraki 305-8573, Japan

Abstract

Methylammonium bismuth iodide, $(CH_3NH_3)_3Bi_2I_9$, is a promising lead-free perovskite active layer for solar cells. In this study, by using gas-assisted deposition method, we have successfully prepared dense and smooth $(CH_3NH_3)_3Bi_2I_9$ active layer, resulting in 25% improvement in V_{OC} (from 0.548 V to 0.686 V) and 17% improvement in efficiency (from 0.070% to 0.082%), compared with the conventional 1-step method.

Keywords: Perovskite solar cells; Lead-free; Bi-based; $(CH_3NH_3)_3Bi_2I_9$; Gas-assisted

1. Introduction

Perovskite solar cells (PSCs) have attracted much attention due to their rapidly-increased and high power conversion efficiency (PCE). Kojima et al. reported the PSCs with conversion efficiency of 3.8 % in 2009 [1]. Within only 7 years, the PCE increased up to 22.1% [2]. The high efficiency is attributed to excellent optical and electrical properties of $CH_3NH_3PbX_3$ (X=I, Br or Cl) [3-5]. However, the $CH_3NH_3PbI_3$ active layer includes toxic Pb; an alternative lead-free active layer is desired. Sn replacement for Pb has been tried to solve this problem [6,7], but durability is the most serious problem in Sn-based PSCs.

Currently, Bi-based perovskite-type compounds gather much attention [8-14]. Among them, $(CH_3NH_3)_3Bi_2I_9$ has high stability in air since Bi^{3+} ions are stable, but the typical PCE of $(CH_3NH_3)_3Bi_2I_9$ PSCs are reported as 0.1-0.2%. Singh et al. have recently reported the 10-week long-term stability of $(CH_3NH_3)_3Bi_2I_9$ PSCs [10], where the performance degradation was only 25% even in the ambient conditions. This result has demonstrated the high stability of $(CH_3NH_3)_3Bi_2I_9$ PSCs. Compared with commonly used perovskites having favorable band gaps, *e.g.* $CH_3NH_3SnI_3$ (~1.3 eV [6]) and $CH_3NH_3PbI_3$ (~1.5 eV [15]), $(CH_3NH_3)_3Bi_2I_9$ has a wider band gap (~2.1 eV [8,13]). $(CH_3NH_3)_3Bi_2I_9$, however, can be an alternative for $CH_3NH_3PbI_3$ due

* Corresponding author: Faculty of Pure and Applied Sciences, University of Tsukuba, Ibaraki 305-8573, Japan.

E-mail address: suzuki@ims.tsukuba.ac.jp (Y. Suzuki).

to the high absorption coefficient ($(CH_3NH_3)_3Bi_2I_9$: 1.1×10^5 cm^{-1} at 500 nm [13], $CH_3NH_3PbI_3$: 1.5×10^4 cm^{-1} at 550 nm [16]). Table S1 summarizes the comparison between $CH_3NH_3PbI_3$ and $(CH_3NH_3)_3Bi_2I_9$.

Since $(CH_3NH_3)_3Bi_2I_9$ has hexagonal unit cell [8,13], it grows into hexagonal plate-like crystals. In previous studies, many pores were found in the perovskite layer, since the perovskite crystals grow perpendicularly or diagonally to the substrate [8-10,12]. Since the morphology of perovskite layer largely affects the cell performance, many researchers have developed cell processing technique to control the perovskite morphology for improving cell performance and reproductivity. In this study, by using gas-assisted deposition method [17], we have prepared a dense and smooth $(CH_3NH_3)_3Bi_2I_9$ active layer to improve the cell performance.

2. Experimental

FTO glass (Pilkington, TEC-7, 7 Ωsq^{-1}) was etched with Zn powder and HCl, and then, was washed by acetone/ethanol. TiO_2 compact layer (electron transport layer, ETL) was deposited by spin-coating at 2000 rpm for 25 s using 20 µl of 0.15 M titanium diisopropoxide bis(acetylacetonate) solution (75 wt% in isopropanol, Sigma Aldrich) diluted by 1-buthanol, and annealed at 125°C for 5 min. Then this process was repeated twice with 0.3 M titanium diisopropoxide bis(acetylacetonate) solution diluted by 1-buthanol. The coated glass was annealed at 500°C for 45 min. After cooling down to room temperature, it was immersed in 0.4 mM $TiCl_4$ aq. solution, followed by annealing at 500°C for 45 min.

The perovskite layer was coated using 1-step method. Perovskite solution was prepared by dissolving BiI_3 (297.9 mg) and CH_3NH_3I (121.4 mg) in DMF (1.0 ml). The perovskite solution (20 µl) was dropped on the pre-heated TiO_2-coated glass at 80°C, and then started spin-coating at 3000 rpm for 20 s with a ramp rate of 1000 rpm/s. For the gas-assisted method, N_2 gas was blown on perovskite solution during the spin-coating. The gas-blow was conducted 4 s after starting spin-coating. After spin-coating, the perovskite film was annealed at 80°C for 10 min. Spiro-OMeTAD solution (13 µl) was spin-coated as a hole-transporting layer (HTL), similarly to our recent paper [18]. Finally, Ag electrode was deposited by thermal evaporation.

The morphology of perovskite and spiro-OMeTAD layers was observed by scanning electron microscopy (SEM, JSM-5600LV, JEOL). The prepared cells were characterized by X-ray diffraction (XRD, Multiflex, Cu-Kα, Rigaku). Optical transmittance of the cells was measured by UV–Vis spectroscopy (UV-Vis, UV-1280, Shimadzu). Current density–voltage (*J*–*V*) characteristics were measured with a solar simulator (XES-40S1, SAN-EI Electric) calibrated to AM 1.5, 100 mW/cm^2 with a standard silicon photodiode (BS-520BK, Bunkokeiki). A black mask was used during the *J*–*V* measurement and the active area was 8.7 mm^2.

3. Results

The perovskite solar cells prepared by the conventional 1-step method and the gas-assisted method are denoted as 'conventional cells' and 'gas-assisted cells,' respectively. Figure 1 shows XRD patterns of conventional and gas-assisted cells. Both cells were composed of $(CH_3NH_3)_3Bi_2I_9$ [8,9,12], FTO (substrate) and Ag (electrode). For the conventional cells, 00*l* preferred orientation was observed.

The results of *J-V* measurement are summarized in Table 1. These data are average of 8 samples measured by back scan. Conventional cells marked 0.070% PCE with J_{SC} of 0.391 mA/cm^2, V_{OC} of 0.548 V and *FF* of 0.33, whereas gas-assisted cells marked 0.082% PCE with J_{SC} of 0.372 mA/cm^2, V_{OC} of 0.686 V and *FF* of 0.32. These PCE values are quite low compared with Pb-based PSCs, but are comparable to those for reported Bi-based PSCs. By gas-assisted method, despite slight decrease of J_{SC}, 25% of significant improvement in V_{OC} was achieved, which resulted in the enhancement of PCE from 0.070±0.0039% to 0.082±0.0021%. The smaller standard error indicates the high reproducibility of gas-assisted method. Figure S1 shows the *J-V* curves of the best performing cells. The gas-assisted cell marked 0.728 V in V_{OC}, which is comparable to the highest V_{OC} in $(CH_3NH_3)_3Bi_2I_9$ PSCs [12].

Figure 2 shows appearances and SEM images of gas-assisted and conventional films. Appearances of the two films are not so different to each other. From SEM observation, the platelet crystals grew perpendicular to the substrate for both methods, however, the density and the surface roughness were completely different. The gas-assisted perovskite layer (Fig. 2(c)) consisted of dense and smooth morphology, whereas the conventional perovskite layer (Fig. 2(d)) was composed of porous and rough morphology of large platelet $(CH_3NH_3)_3Bi_2I_9$ crystals. The perovskite morphology of conventional method corresponds with the previous reports [8-10,12].

The spiro-OMeTAD layer (HTL) coated on the gas-assisted perovskite (Fig. 2(e)) fully covered the whole area, whereas that on the conventional perovskite (Fig. 2(f)) contained many pores. With the long-term perspective, in case of having pores in HTL, perovskite will be decomposed by moisture through pores. Furthermore, through the channel of pores in HTL, I^- ions from the perovskite layer would erode the Ag electrode directly contacting with perovskite layer, resulted in the formation of AgI, and resulted in decline of the durability and performance. Taking these points into consideration, the gas-assisted method is favorable for depositing $(CH_3NH_3)_3Bi_2I_9$ anisotropic crystals.

Figure 3 shows the UV-Vis spectra. Absorbance edge was ~600 nm, as reported in the references [10,12]. The absorbance and the transmittance of both cells were similar to each other, which resulted in the similar J_{SC} values, but slightly higher J_{SC} value (Table 1) and opaque appearance (Fig. 2(b)) for the conventional cells can be explained by the light scattering effect

by the surface texture.

4. Discussion

The charge recombination processes can be categorized in three types: (1) deactivation of electrons in perovskite layer, (2) recombination at ETL/perovskite/HTL interfaces and (3) recombination at ETL/HTL interface (i.e., direct contact between ETL and HTL). As for (1), considering that the charge diffusion length is limited, when the electrons are generated far from ETL, the electrons tends to be recombined in perovskite layer. The perovskite layer in the gas-assisted cells was somewhat thinner than that in the conventional cells, and hence, the electron injection to the ETL should be more efficient for the gas-assisted cells. As for (2), since the perovskite layer in the gas-assisted cells was dense and smooth, coverage ratio as well as adhesion between the perovskite layer and HTL were further improved. As for (3), the SEM observation did not give the evidence of ETL/HTL direct contact, but at least, the ETL was fully covered with perovskite layer in gas-assisted cells. From these considerations (1)-(3), improvement in V_{OC} for the gas-assisted cells is attributable to the suppression of charge recombination. Carrier life-time measurement will be effective for $(CH_3NH_3)_3Bi_2I_9$ PSCs in the future.

5. Conclusions

The average PCE prepared by the gas-assisted method was 0.082% (Jsc=0.372 mA/cm^2, Voc=0.686 V, FF=0.32), which is superior to that of the conventional 1-step method, 0.070% (Jsc=0.391 mA/cm^2, Voc=0.548 V, FF=0.33). Preparing dense and smooth Bi-based perovskite layer by gas-blowing probably lead to low charge recombination, which resulted in 25% improvement in V_{OC}. The maximum V_{OC} (0.728 V) in this study is comparable to that of the best V_{OC} in planer-type $(CH_3NH_3)_3Bi_2I_9$ cell ever reported. Even if the perovskite layer is composed of anisotropic materials like $(CH_3NH_3)_3Bi_2I_9$, the gas-assisted method is a promising way to enhance PCE by preparing dense and smooth perovskite layer.

Acknowledgment

We thank to Prof. Kadowaki and Prof. Kashiwagi for the use of vacuum vapor deposition system, and to Prof. Tamotsu Koyano (Cryogenics Division, Research Facility Center, University of Tsukuba) for his help on SEM observation.

References

[1] A. Kojima, K. Teshima, Y. Shirai, T. Miyasaka, J. Am. Chem. Soc. 131 (2009) 6050-6051.

[2] Research cell efficiency records. (http://www.nrel.gov/pv/assets/images/efficiency_chart.jpg), (accessed November 2016).

[3] S.D. Stranks, G.E. Eperon, G. Grancini, C. Menelaou, M.J.P. Alcocer, T. Leijtens, L.M. Herz, A. Petrozza, H.J. Snaith, Science 342 (2013) 341-344.

[4] C. Wehrenfennig, G.E. Eperon, M.B. Johnston, H.J. Snaith, L.M. Herz, Adv. Mater. 26 (2014) 1584-1589.

[5] W.-J. Yin, T. Shi, Y. Yan, Adv. Mater. 26 (2014) 4653-4658.

[6] N.K. Noel, S.D. Stranks, A. Abate, C. Wehrenfennig, S. Guarnera, A.-A. Haghighirad, A. Sadhanala, G.E. Eperon, S.K. Pathak, M.B. Johnston, A. Petrozza, L.M. Her, H.J. Snaith, Energy Environ. Sci. 7 (2014) 3061–3068.

[7] F. Hao, C.C. Stoumpos, D.H. Cao, R.P.H. Chang, M.G. Kanatzidis, Nat. Photonics. 8 (2014) 489–494.

[8] B.W. Park, B. Philippe, X. Zhang, H. Rensmo, G. Boschloo, E.M. Johansson, Adv Mater. 27 (2015) 6806-6813.

[9] M. Lyu, J.-H. Yun, M. Cai, Y. Jiao, P.V. Bernhardt, M. Zhang, Q. Wang, A. Du, H. Wang, G. Liu, L. Wang, Nano Res. 9 (2016) 692-702.

[10] T. Singh, A. Kulkarni, M. Ikegami, T. Miyasaka, ACS Appl. Mater. Interfaces, 8 (2016) 14542–14547.

[11] S. Öz, J.-C. Hebig, E. Jung, T. Singh, A. Lepcha, S. Olthof, F. Jan, Y. Gao, R. German, P.H.M. van Loosdrecht, K. Meerholz, T. Kirchartz, S. Mathur, Solar Energy Mater. Solar Cells 158 (2016) 195-201.

[12] X. Zhang, G. Wu, Z. Gu, B. Guo, W. Liu, S. Yang, T. Ye, C. Chen, W. Tu, H. Chen, Nano Res. 9 (2016) 2921-2930.

[13] K. Eckhardt, V. Bon, J. Getzschmann, J. Grothe, F.M. Wisser, S. Kaskel, Chem. Commun. 52 (2016) 3058-3060.

[14] A.J. Lehner, D.H. Fabini, H.A. Evans, C.-A. Hébert, S.R. Smock, J. Hu, H. Wang, J.W. Zwanziger, M.L. Chabinyc, R. Seshadri, Chem. Mater. 27 (2015) 7137–7148.

[15] H.S. Kim, C.R. Lee, J.H. Im, K.B. Lee, T. Moehl, A. Marchioro, S.J. Moon, R.H. Baker, J.H. Yum, J.E. Moser, M. Grätzel, N.G. Park, Sci. Rep. 2 (2012) 591.

[16] J.H. Im, C.R. Lee, J.W. Lee, S.W. Park, N.G. Park, Nanoscale 3 (2011) 4088–4093.

[17] Y. Dkhissi, F. Huang, S. Rubanov, M. Xiao, U. Bach, L. Spiccia, R.A. Caruso, Y.B. Cheng, J. Power Sources 278 (2015) 325–331.

[18] Y. Okamoto, Y. Suzuki, J. Phys. Chem. C 120 (2016) 13995−14000.

Table

Table 1 Average photovoltaic performances of back scan for conventional and gas-assisted cells.

Sample	J_{sc} (mA/cm²)	V_{oc} (V)	*FF*	PCE (%)
Conventional	0.391	0.548	0.33	0.070
Gas-assisted	0.372	0.686	0.32	0.082

Figures

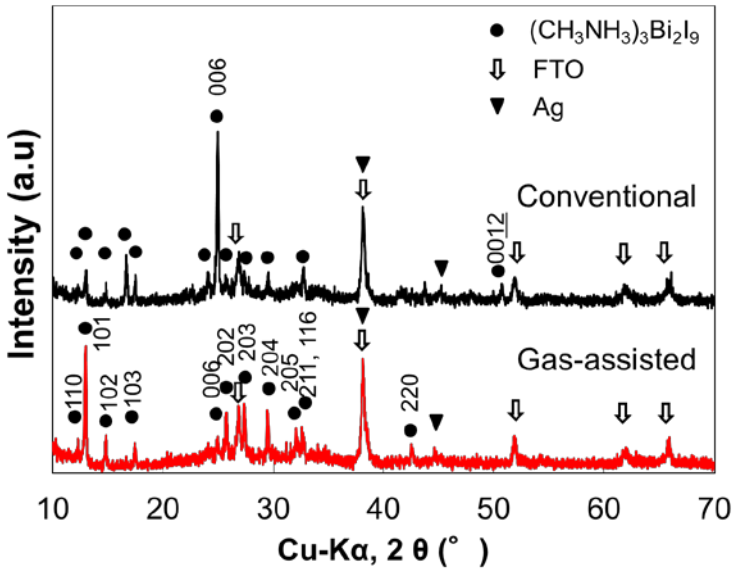

Fig. 1 XRD patterns of conventional and gas-assisted cells. Space group of $(CH_3NH_3)_3Bi_2I_9$: $P6_3/mmc$ (No. 194).

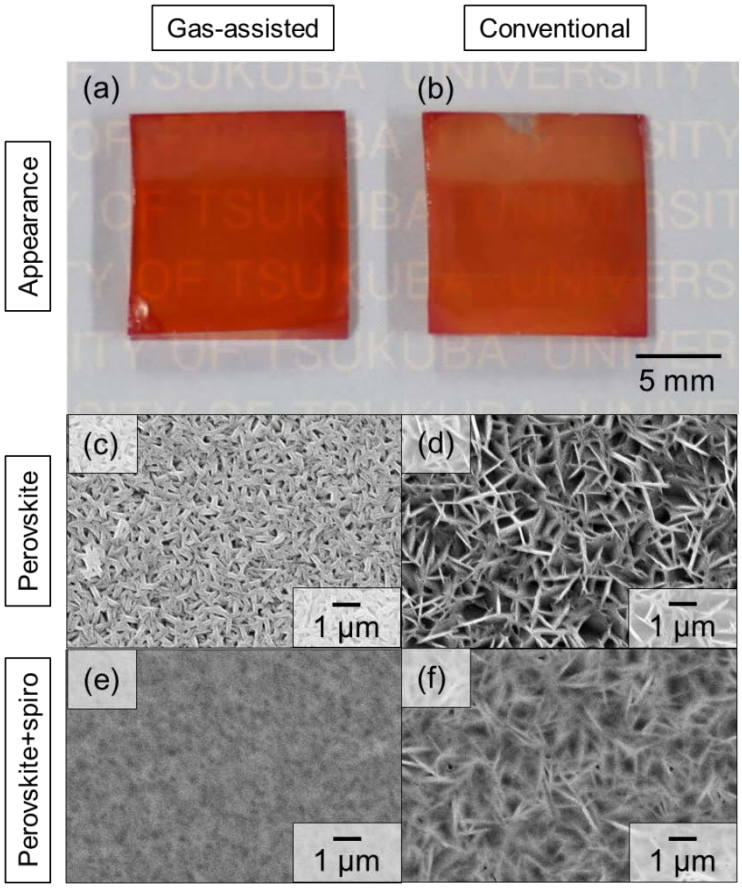

Fig. 2 Appearances and SEM images of (a, c, e) gas-assisted and (b, d, f) conventional films

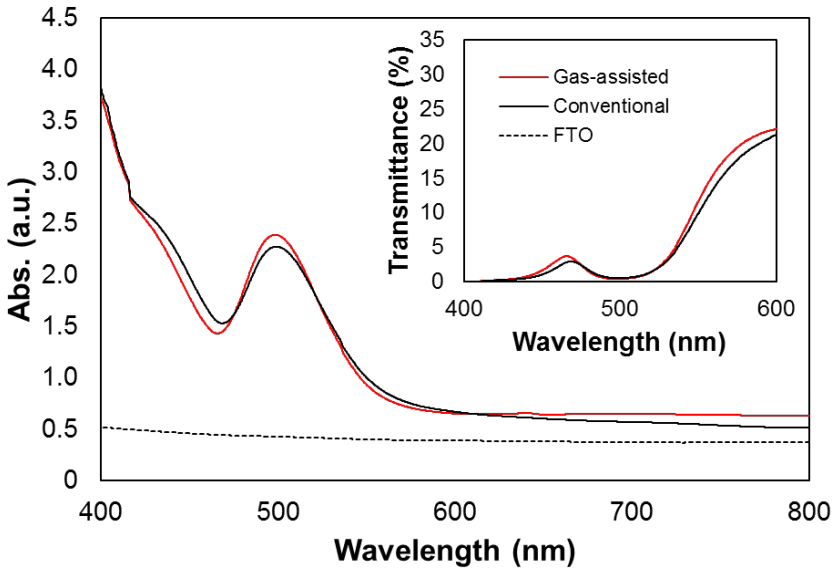

Fig. 3 UV-Vis spectra of conventional and gas-assisted cells.